An Improved Method for InSAR Atmospheric Phase Correction in Mountainous Areas

Mengyao Shi, Junhuan Peng, Xue Chen, Yueze Zheng, Honglei Yang, Yuhan Su, Guoya Wang, and Wenwen Wang

***Abstract*—Time series interferometric synthetic aperture radar (TS-InSAR) has been a powerful tool for monitoring land surface deformation over the last two decades. Atmospheric effects cause large-scale delays in InSAR observations, which is one of the difficulties facing deformation calculations from differential InSAR and time-series InSAR. Currently, the atmospheric delay is derived mainly from auxiliary data from sources such as the global navigation satellite system (GNSS) and moderate-resolution imaging spectroradiometry (MODIS), but GNSS data are limited by the sparse distribution of observation stations. MODIS data may also not temporally match SAR image acquisition, which leads to low accuracy in atmospheric phase correction. This article presents a decomposition method to remove the atmospheric delay. We consider the atmospheric phase to be caused by the combined changes in spatial position and elevation. Therefore, quadtree segmentation is applied to divide the topographic units, and we improve the drift function of universal kriging by adding an elevation component. We then interpolate the whole atmospheric phase space from reliable sampling points estimated by the coherence coefficient. Using Sentinel-1 data, we test the proposed method in discriminating and monitoring a mining subsidence area in Shanxi Province and compare the results with the results from interferometric point target analysis and the network-based variance-covariance estimation method. The results demonstrate that the proposed method is superior to existing methods for the detection of deformation inverted from TS-InSAR.**

Manuscript received February 10, 2021; revised June 5, 2021 and August 24, 2021; accepted September 12, 2021. Date of publication September 20, 2021; date of current version October 27, 2021. This work was supported by the National Natural Science Foundation of China under Grant 42074004 and in part by Shanxi Transportation Holdings Group, Company, Ltd., under Grant 19-JKKJ-3. (*Corresponding author: Mengyao Shi.*)

Mengyao Shi is with the School of Land Science and Technology, China University of Geosciences, Beijing 100083, China (e-mail: shimengyao@cugb.edu.cn).

Junhuan Peng is with the School of Land Science and Technology, China University of Geosciences, Beijing 100083, China, and also with the Shanxi Key Laboratory of Resources, Environment and Disaster Monitoring, Jinzhong 030600, China (e-mail: pengjunhuan@163.com).

Xue Chen is with the School of Land Science and Technology, China University of Geosciences, Beijing 100083, China, and also with the Department of Geosciences, University of Padua, I-35131 Padua, Italy (e-mail: chenxue@cugb.edu.cn).

Yueze Zheng is with the Beijing Institute of Surveying and Mapping, Beijing 100038, China (e-mail: zheng_cugb@163.com).

Honglei Yang and Yuhan Su are with the School of Land Science and Technology, China University of Geosciences, Beijing 100083, China (e-mail: hongleiyang@cugb.edu.cn; s_yuhan@163.com).

Guoya Wang is with the Geological Hazards Prevention Institute, Gansu Academy of Sciences, Lanzhou 730000, China (e-mail: guoya@lzb.ac.cn).

Wenwen Wang is with the Shanxi Key Laboratory of Resources, Environment and Disaster Monitoring, Jinzhong 030600, China, and also with the Coal Geological Geophysical Exploration Surveying and Mapping Institute of Shanxi Province, Jinzhong 030600, China (e-mail: 530619120@qq.com).

Digital Object Identifier 10.1109/JSTARS.2021.3113619

***Index Terms*—Atmospheric phase correction, interferometric synthetic aperture radar (InSAR), kriging interpolation method.**

I. Introduction

INTERFEROMETRIC synthetic aperture radar (InSAR) is a new technology for monitoring surface deformation that processes two complex images obtained by a satellite passing a single location at two moments in time to calculate the phase change caused by deformation; in this way, the characteristics of surface deformation can be analyzed. InSAR has been successfully used in many fields to study phenomena such as landslides, ground subsidence, and earthquakes; in addition, this technique is regarded as an effective method for the dynamic monitoring and extent identification of subsidence in mining areas. However, when a satellite transmits electromagnetic waves through the atmosphere, the transmission delay due to a large quantity of water vapor can produce a deviation in the converted distance of up to 2.8 cm on one path in desert areas [2]. Owing to differential interferometric data processing, the phase changes caused by such differences in the atmospheric distribution of water vapor affect the extraction of elevation data and the calculation of deformation. According to previous studies, a 20% change in relative humidity leads to errors of 10–14 cm in deformation or deviations of 80–290 m in elevation [3]. In addition, the effects of atmospheric disturbances on interferograms change rapidly and show different characteristics over large areas (see Fig. 1). In particular, the large magnitudes of atmospheric delays mask the deformation phase [see Fig. 1(a)]. Therefore, atmospheric change is an important error source in differential interferometry. Moreover, the topography of mining areas is complex and diverse, and the changes in the atmosphere over these areas are severe; thus, performing atmospheric correction in mining areas is important for the dynamic monitoring of subsidence.

Recently, many scholars have explored tropospheric correction methods in interferometry. Excluding weather models, the existing correction methods can be roughly divided into the following two categories: interpolation methods and time-series methods. Interpolation methods are simple techniques, wherein auxiliary data from sources such as the global navigation satellite system (GNSS) or medium-resolution imaging spectrometry (MERIS/MODIS) and other meteorological data are interpolated to calculate the zenith wet delay [4]–[6]. In contrast, time-series methods entail InSAR data processing and consider the temporal and spatial characteristics of the atmosphere or

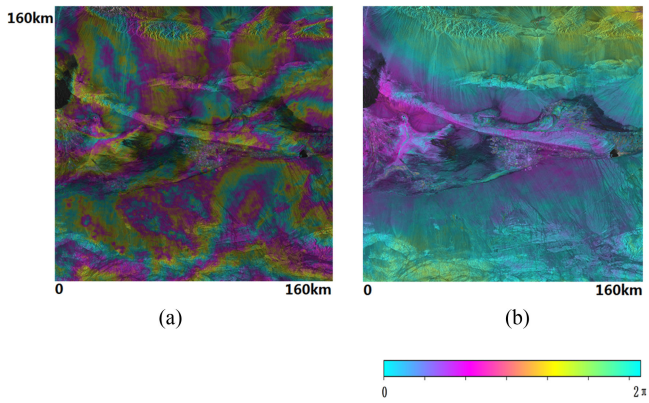

Fig. 1. Atmospheric effects in interferograms. (a) Interferogram from 3 June 2017 to 13 October 2017. (b) Interferogram from 30 December 2017 to 24 November 2017.

the relationship between the atmospheric phase and the elevation by employing methods such as the small baseline subset (SBAS) technique and permanent scatterer (PS) method [3], [7], [8].

The interpolation method is a straightforward approach that estimates the zenith wet delay to invert the water vapor content and does not require the analysis of the temporal or spatial characteristics of the atmosphere. A reasonable interpolation method should be applied to generate the atmospheric correction in an area when the number of observation points is sparse. Common interpolation methods include inverse distance weighted (IDW) interpolation and kriging interpolation. Samir *et al.* [4] proposed a novel interpolation method using three-dimensional inverse distance weighting based on evidence of a strong correlation between elevation and water vapor variations. Hu *et al.* [5] utilized cubic spline interpolation on grid points from sea level to a reference elevation for the temperature, pressure, and relative humidity along the vertical direction; this approach provides horizontal interpolation on the desired locations along the line-of-sight direction. Yu *et al.* proposed a method that uses GNSS data to reduce tropospheric effects and an iterative model with elevation data to separate tropospheric stratified and turbulence components [6], [7]. Yu *et al.* [8] proposed an atmospheric correction model named the generic atmospheric correction online service (GACOS) for InSAR and released the products, which are based on a fusion of GNSS measurements and ECMWF weather models with an iterative tropospheric decomposition mode. IDW interpolation employs the weighted sum of all known points in space to estimate the values of unknown points, where the weight depends on the reciprocal of the distance or the squared distance [9]. Due to the low density of meteorology stations, GNSS stations, and MODIS data, the resolution of which is only 1000 m, the resolution of external data is far less than that of SAR images (meter level); this poor resolution introduces error when interpolating in a wide area with a variable atmospheric water vapor distribution [10]–[12]. In addition, interpolation on the global scale depends on the spatial distribution of spatial attributes [13], [14]. Hence, this interpolation method, which uses only an inverse proportional function to describe spatial attributes, is not sufficiently accurate. In contrast, kriging interpolation depends on a mathematical model, and a statistical model (e.g., the Matern variogram model) is better than the spherical variogram model in some cases [15]. The latter model requires a large number of SAR images to resolve the temporal and spatial distributions. The stacking method generates an interferogram stack to reduce the time decorrelation phase, such as that due to noise and atmospheric effects; for example, the SBAS and PS methods apply a temporal high-pass filter and spatial low-pass filter to reduce the atmospheric phase from the mixed interferometric phase [16]. Werner *et al.* [22] presented a method named interferometric point target analysis (IPTA) to calculate the target points in multiple interferometric images by applying statistical regression analysis, which is an extension of traditional PS InSAR and SBAS InSAR, thereby providing a greater data processing efficiency and data storage capacity [23]. In this method, a high-coherence point grid is established during repeated iterative analysis and the correction of the unwrapped phase to separate the surface deformation information. The atmospheric signal related to the topography should be removed by the component related to the perpendicular baseline, while the other atmospheric signals should be estimated by spatial filtering of the nonlinear component.

Tropospheric delays are commonly considered a mixture of turbulence delays and stratified delays [17]. Considering the characteristics of the above two components, Wei *et al.* [18] decomposed the atmospheric phase into terrain-related components and turbulence components, which were modeled and estimated by least squares (LS) estimation and the spatial variation model, respectively, achieving good results, but the influence of the elevation error was ignored in the modeling. In addition, Li *et al.* [19] and Cao *et al.* [20] proposed a network-based estimation method to model the spatiotemporal variation in tropospheric signals and to estimate the temporal variance-covariance matrix of time-series InSAR (TS-InSAR) observations. In this method, the undifferentiated atmospheric signals for each SAR acquisition are assessed. In addition, the atmospheric signals related to the topography are removed, and the deformation region is masked in advance. However, this method adopts only a spherical model to model the spatial variance of samples, and the spatial distribution of the phase space is not analyzed further.

Therefore, combining the advantages of the interpolation and time-series atmospheric correction methods mentioned above, this article proposes an improved atmospheric correction method. In this method, a quadtree segmentation method is used to segment the digital elevation model (DEM) to obtain fluctuating topographic points as sampling points for kriging interpolation. The spatially heterogeneous atmospheric phase is interpolated by the universal kriging interpolation method with an improved drift function. In addition, Sentinel-1 data are utilized to monitor a mining subsidence area in Shanxi Province to verify the proposed method.

The rest of this article is organized as follows. Section II introduces the method for decomposing the atmospheric phase and the proposed method for correcting the spatially heterogeneous atmospheric phase, including the improved universal

kriging method. Section III describes an example to analyze the reliability of the proposed method. Finally, Section IV concludes this article.

II. Method

A. Atmospheric Phase Decomposition of InSAR

The atmosphere is a layer containing mixed gases enveloping the surface of the Earth. At middle latitudes, the average altitude of the troposphere, more than 90% of which is water vapor, is 10–12 km. Because temperature varies with elevation, water vapor is unevenly distributed in the vertical and horizontal directions, i.e., the atmosphere is spatially heterogeneous, which affects electromagnetic wave propagation. In addition, there are many free electrons above the troposphere that also affect electromagnetic wave propagation and, thus, long-wavelength SAR sensors due to the dispersive property of the ionospheric medium. When an electromagnetic wave penetrates the troposphere, which is enriched in water vapor, the propagation path necessarily bends, and the transmission time is delayed [17].

The variation in the atmospheric distribution of water vapor between two repeated observations leads to a differential atmospheric delay phase that cannot be eliminated by differential interferometry. In addition, because the refractive index in space is anisotropic, the corresponding atmospheric phase change can be divided into two directions: horizontal and vertical. The change in the horizontal direction is due to the turbulent field, while that in the vertical direction is due to the stratified atmosphere related to the elevation.

1) Stratified Atmosphere: Based on the characteristics of differential InSAR (D-InSAR), the interferometric phase includes the following main phases: the deformation phase, terrain phase, baseline phase, atmospheric phase, and noise phase. These phases are additive. The terrain phase and baseline phase can be reduced by external DEM data and precise orbit or ground control points, respectively [24]. After correcting these phases, the interferometric phase includes only a mixture of the deformation, atmosphere, and noise phases. However, the vertically stratified atmosphere can be considered a function of elevation. Taylor and Peltzer [25] pointed out that there is a linear or exponential relationship between the atmospheric delay phase and elevation.

To show the difference between the two abovementioned relationships, we take the study area as an example. A comparison reveals that the exponential model fits better than the linear model in mountainous areas (see Fig. 2). The R^2 values of the exponential model and the linear model are 0.2068 and 0.1698, respectively, mainly because mountainous areas present undulating topography, which is difficult to fit with a linear model. Generally, the vertically stratified atmosphere is obvious and significant in areas with large topographic changes.

2) Horizontal Atmospheric Turbulence: Horizontal atmospheric turbulence is caused mainly by the spatial and temporal distributions of water vapor, which is spatially heterogeneous. In addition, atmospheric noise is uncorrelated in time. Therefore, the spatial statistics method can be used to extract the horizontal

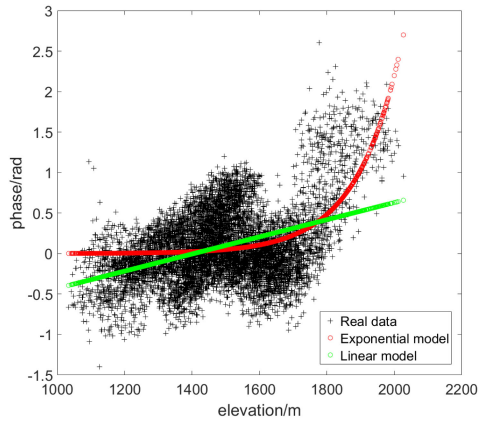

Fig. 2. Regression results (black crosses: observations; red circles: exponential model results; green line: linear model results).

atmospheric turbulence component, which is independent of the terrain. The most common interpolation methods are IDW interpolation [26] and kriging interpolation [27]. The former uses the weighted sum of all known points in space to estimate the values of unknown points, where the weight depends on the reciprocal of the distance. In addition, IDW is a nonparametric method that relies on previous experience to set appropriate weights and windows.

However, it is not accurate to describe the spatial information using only an inverse ratio function, especially with an uneven distribution of known points, because excessively sparse observation points often lead to errors in the interpolation results. In contrast, kriging interpolation is a parametric method using a regression algorithm for spatial modeling and the interpolation of random fields according to the variogram function of spatial variables based on minimum variance; this technique can provide optimal unbiased linear estimations and has a stable prediction effect for specific stochastic processes [28]. Compared with that of IDW, the kriging weight decreases with the characteristics of the variogram rather than the distance. Knospe and Jonsson [15] used kriging interpolation embedded with the Matern variogram model and found good agreement between the physical and statistical characteristics of the atmospheric phase and the spatial atmospheric refractive index obeying the Kolmogorov power law of turbulence. However, considering the anisotropy of the atmosphere, more parameters increase the complexity of the model; thus, this method is suitable only for dense sampling [19]. We choose some columns and rows of a differential phase with the topographic phase removed and a flattened phase in the study area. The azimuth and range pixel scatter diagrams show that after unwrapping the phase map with the masked deformation area, the phase intrinsically tends to change (see Fig. 2), which means that the variable exhibits drift in the range, azimuth, and vertical directions due to the influence of the tropospheric delay. Due to the spatial anisotropy of the atmosphere, the variable mean value and nonstationary variance show that the results do not satisfy second-order stationarity or the principle of the original kriging method. The display of phase

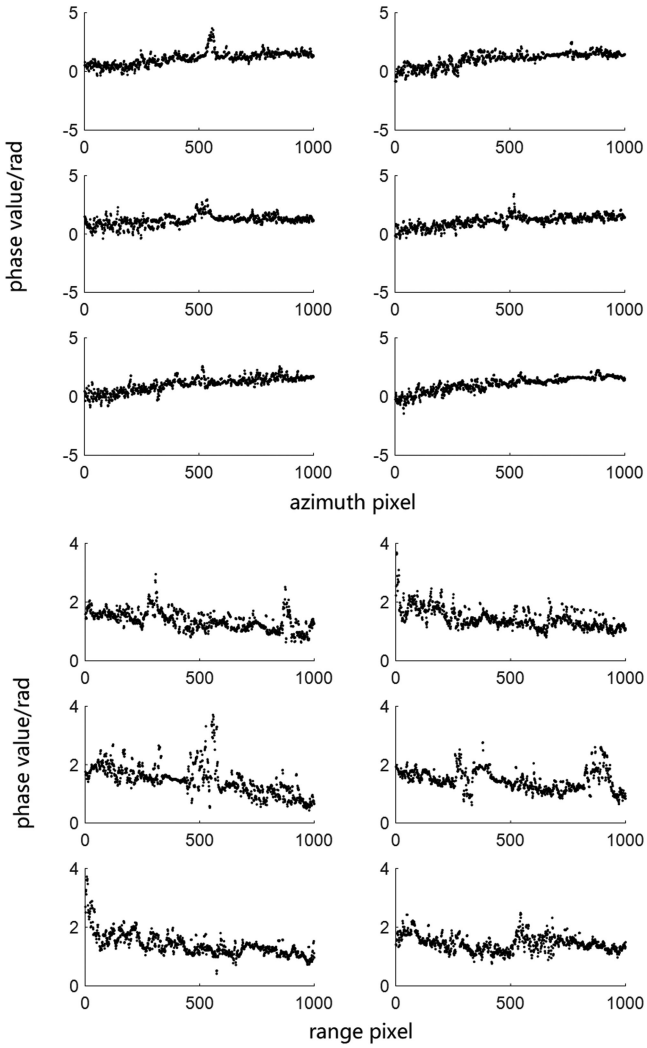

Fig. 3. Scatter diagrams of pixels in the azimuth and range directions. The *X*-axis shows the number of points in the azimuth or range direction, and the *Y*-axis shows the phase value of each point.

values in different directions indicates that the trend changes are inherent (see Fig. 3).

B. Modeling and Estimation of the Atmospheric Phase

Therefore, universal kriging should be used for the spatially heterogeneous atmosphere. For two points x and y on the surface, their interferometric phase φ can be expressed as

$$\varphi\ (x)\ = \mathcal{F}(x) + z\,(x) \tag{1}$$

$$\mathrm{E}\varphi\ (x)\ = \mathcal{F}\,(\mathrm{x}) \tag{2}$$

$$\mathrm{V}[\varphi\,(x) - \varphi\,(y)] = 2\gamma\,(\mathrm{x},\mathrm{y}) \tag{3}$$

where E is the mathematical expectation; V is the variance; γ is a variogram function; $\mathcal{F}$ is a drift function, usually expressed as a polynomial function; and z is a regionalization variable with zero expectation that can be regarded as a random oscillation around $\mathcal{F}$. The variogram function is usually of one of the following types: spherical, exponential, mixed exponential, Gaussian, linear, power function, or spline type. Different types

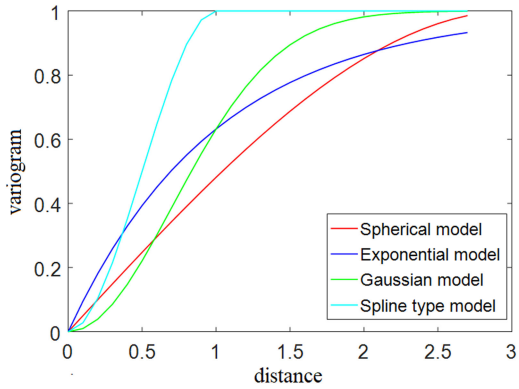

Fig. 4. Diagram of different types of standard variogram models.

correspond to the changing characteristics of different variables and the rate change in the variogram function with increasing distance (see Fig. 4).

Therefore, if a suitable variogram model is selected, the spatial statistical information can be used to describe the characteristics of the spatially heterogeneous atmosphere, and the atmospheric phase of an unknown point can be estimated by the atmospheric phase of the known point.

In this article, we propose a method for spatially heterogeneous atmospheric phase modeling that can estimate the TS-InSAR interferometric phase. Through the SBAS method, an interferometric pair is constructed according to the time and baseline thresholds. Following differential interferometry, the terrain phase and the baseline phase in the unwrapped phase are eliminated, and thus, only the atmospheric phase, terrain residual phase, deformation phase, and noise phase are included in the phase map. According to the description above, we establish a general model to estimate the stratified atmosphere and horizontal atmospheric turbulence phases. Considering the relationship between the DEM and the stratified atmosphere, we introduce elevation h into the initial universal kriging interpolation model. Based on the above equations, the atmospheric unwrapped phase is modeled as

$$\varphi\ =\ \mathcal{F}\,(x, y, h) + \varphi_e \tag{4}$$

where φ is the unwrapped phase; h is the elevation; x, y are the coordinates; $\mathcal{F}(x,\ y,\ h)$ represents the atmosphere, which is related to the location and elevation; and φ_e is the residual phase, including the deformation information and noise. The function is added to the drift function of the universal kriging model to perform the regression, which is shown in (7). In other words, the stratified atmospheric phase and the horizontal turbulent atmospheric phase are estimated simultaneously in this function instead of through stepwise calculation. The proposed method of atmospheric phase correction is shown as follows.

1) Identification and Sampling of the Atmospheric Region: Through the stacking method, which considers the correlated spatial distribution and uncorrelated temporal distribution of the turbulent atmosphere, the phase of continuous deformation in the mean phase becomes obvious. Moreover, the average atmospheric phase is not significant due to the temporal averaging

process when the number of images is sufficient [17]. In this way, the deformation region is excluded because the deformation process and location are continuous. Considering the accuracy of the sampling points, the known points in the atmospheric region are reselected by coherence. Therefore, the coherence coefficient of all the points should be considered to extract reliable information on the phase value.

Choosing a region with good coherence can eliminate the occurrence of random and unreliable points in the interferogram. In addition, the density of sampling points is reduced; thus, the speed of the interpolation operation increases. Aiming at processing *N* interferograms for SBAS interferometry, we calculate the mean phase in the time domain.

$$V = \frac{\sum_1^k \phi_i}{k}, \quad i = 1, \ldots, k \\ (1 < k < n, \ k \text{ is positive integer}) \tag{5}$$

where *V* is the average phase and ϕ_i is the phase of the *i*th interferogram.

Kriging interpolation utilizes the variograms calculated by all the known sampling points to interpolate the whole phase space. In other words, dense sampling may not improve the interpolation accuracy and may require considerable time. According to the phase model mentioned above, the values of the sampling points include horizontal and vertical information. To sample the spatial information effectively, a quadtree method is used to separate the DEM into tree structures of different levels for the querying of different elevation changes [29]. In this algorithm, the whole space is first divided into four subblocks. If the statistical characteristics (i.e., mean and variation) of a block are greater than the threshold values or the number of subblocks is smaller than the default, the block is further segmented. Then, we choose the centers of the final blocks as the sampling points because every sampling point represents its local elevation. This sampling method ensures that the sampling points represent the whole phase space and that the points in areas with elevation gradient variations are densified. Compared with the traditional moving window uniform sampling method, which generates a small window and takes the most stable point in the window as the known point, the quadtree segmentation method makes more effective use of the spatial distribution information and improves the calculation efficiency.

2) Kriging Interpolation: The kriging method assumes that the distance or direction between sampling points can reflect the spatial correlation, which can be used to explain the surface changes. The kriging method can fit a mathematical function to a specified number of points or all points within a specified radius to determine the output value of each location. Universal kriging is an unbiased multiple regression estimation method with drift and fluctuations in the spatial variable. Considering the selection of the abovementioned stratified atmospheric model, the proposed method adds the exponential model into the drift function of universal kriging interpolation. Thus, (4), which expresses the stratified and horizontal turbulent atmospheric phases, can be expressed specifically as

$$\boldsymbol{\varphi}(\boldsymbol{x}) = \mathcal{F}\boldsymbol{\lambda}, \boldsymbol{x}, \boldsymbol{h}) + \boldsymbol{z}(\boldsymbol{x}) \tag{6}$$

$$\begin{aligned} \mathcal{F}(\boldsymbol{\lambda}, \boldsymbol{x}, \boldsymbol{h}) &= \lambda_1 f_1(x) + \ldots \\ &\quad + \lambda_{p-2} f_{\mathrm{p-2}}(x) + \lambda_{p-1} \mathrm{e}^{\lambda_p h} \\ &= \boldsymbol{f}(\boldsymbol{x})^{\boldsymbol{T}} \end{aligned} \tag{7}$$

where λ is the weight coefficient, *h* is the elevation, *p* is the number of polynomials in drift $\mathcal{F}$, and $z(x)$ denotes the fluctuation with zero expectation that can be regarded as a random oscillation around $\mathcal{F}$.

Through modeling, it is found that the coefficient matrix of the Gauss–Markov model also contains random errors. And the LS solution in vertically stratified atmosphere matching is not optimal but biased [28]. Therefore, the errors-in-variables (EIV) model is applied as an adjustment model to consider the errors of the observation vector and coefficient matrix at the same time. The corresponding adjustment method is total LS and the EIV model with errors can be expressed as

$$\mathrm{f} - \boldsymbol{e_f} = (\boldsymbol{A} - \boldsymbol{E_A})\ \boldsymbol{x} \tag{8}$$

where f is the observation vector with the random error e_f, A is the coefficient matrix with the random error E_A, and x is the parameter vector to be solved. The random error has the following statistical properties:

$$\begin{bmatrix} \boldsymbol{e_f} \\ \boldsymbol{E_A} \end{bmatrix} = \begin{bmatrix} \boldsymbol{e_f} \\ \mathbf{vec}(\boldsymbol{E_A}) \end{bmatrix} \\ \begin{pmatrix} 0 \\ 0 \end{pmatrix}, \sigma_0^2 \begin{bmatrix} \boldsymbol{Q_f} & 0 \\ 0 & \boldsymbol{Q_A} \end{bmatrix} \tag{9}$$

where vec is the operator of the matrix column vectorization and the coefficient matrix can be expressed as $\boldsymbol{Q_f} = \boldsymbol{P_f^{-1}}$, $\boldsymbol{Q_A} = \boldsymbol{P_A^{-1}}$. Under the total LS criterion, parameter estimation considering the error of the coefficient matrix can be achieved through iteration as

$$\boldsymbol{e_f^T P_y e_f} + \boldsymbol{e_A^T P_A\ e_A} = \ \min \tag{10}$$

$$\hat{\boldsymbol{v}}^{i+1} = \left(\boldsymbol{f} - \boldsymbol{A}\hat{x}^i\right)^T \ \left(\boldsymbol{f} - \boldsymbol{A}\hat{x}^i\right)\left(1 + \hat{\boldsymbol{x}}^{i\ T}\hat{\boldsymbol{x}}^i\ \right)^{-1} \tag{11}$$

$$\hat{\boldsymbol{x}}^{i+1} = \left(\boldsymbol{A}^T\boldsymbol{A}\right)^{-1}(\boldsymbol{A}^T\boldsymbol{f} + \hat{\boldsymbol{x}}^i\hat{\boldsymbol{v}}^{i+1}) \tag{12}$$

where $\hat{v}^{i+1}$ are the residuals of observations obtained by the $(i+1)$th iteration and $\hat{x}^{i+1}$ is the parameter estimate obtained by the $(i+1)$th iteration. The iteration ends when $||\hat{x}^{i+1} - \hat{x}^i|| < \varepsilon$ (ε is a minimum number), and the initial value of $\hat{x}^i$ is the LS solution.

$$\hat{\boldsymbol{x}}^0 = \left(\boldsymbol{A^T A}\right)^{-1}\boldsymbol{A^T y} \tag{13}$$

The corresponding covariance function can be expressed as

$$COV\left[\boldsymbol{z}(\boldsymbol{w})\,\boldsymbol{z}(\boldsymbol{x})\right]\sigma^2\ R(d, w, x) \tag{14}$$

where COV is the covariance function, σ^2 is the variance of the fluctuation z, *w* is the sampled known point, and *x* is the point to be interpolated. *R* is the correction model with the distance d of the variogram mentioned in (3). At this point, the variogram *R* should be chosen to adapt to the spatial variation of the spatially heterogeneous atmosphere before the interpolation step. After universal kriging interpolation, the atmospheric phase can be calculated.

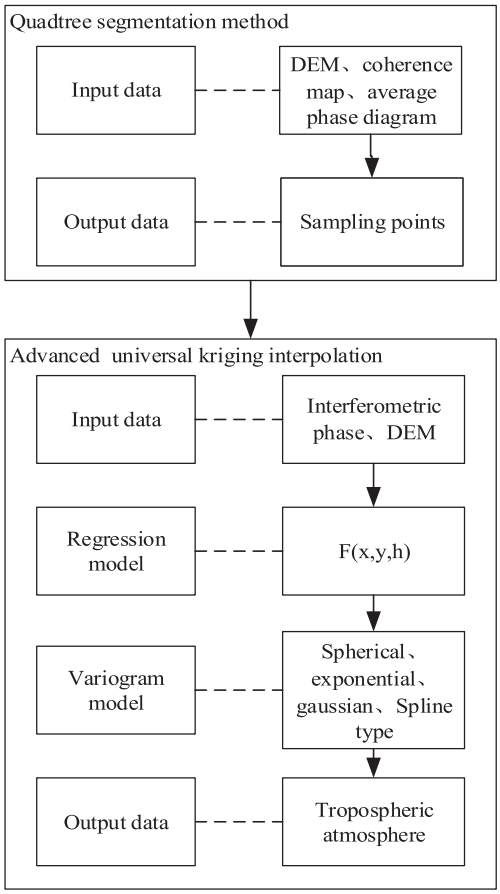

Fig. 5. Flowchart of atmospheric phase correction.

3) Estimating the Atmospheric Phase: Based on the processes above, the position, elevation, and unwrapped phase of the extracted sampling points are introduced, and the advanced regression model and variogram model are used to interpolate the whole interferogram phase space. Since the height residual and noise phase are high-frequency signals in space, this result can be regarded as the atmosphere by kriging interpolation equivalent average weighting [30]. The overall process is shown in Fig. 5.

III. Results

A. Case Study

The study area is located in Changzhi city in Shanxi Province, China (see Fig. 6). To test the proposed method, 84 Sentinel-1 satellite images are used. Detailed information on the data is listed in Table II.

Due to the complex terrain and the distribution of mountains and valleys in the study area, the water vapor varies dramatically, which affects the InSAR monitoring of coal mining subsidence areas. Therefore, the atmospheric delay of all interferograms must be corrected to improve the deformation monitoring accuracy in coal mining subsidence areas.

To do so, we first adaptively divide the DEM into small blocks according to the elevation gradient with the quadtree

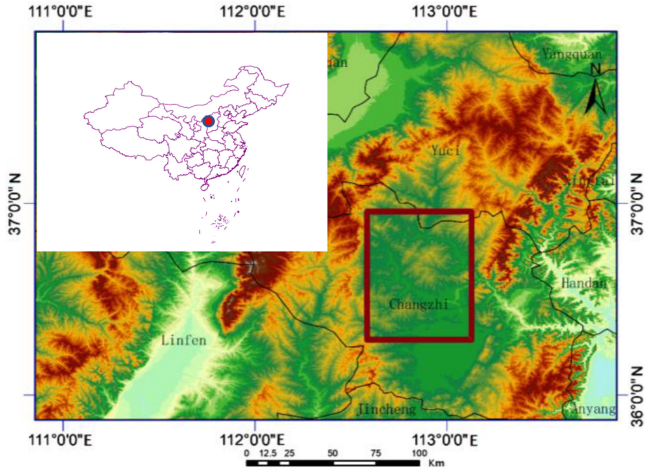

Fig. 6. Location of the study area. The red rectangle shows the extent of data coverage.

TABLE I
Comparison Between the Quadtree and Uniform Window Methods in the Experiment

	Quadtree	4*4 uniform window
Number of points	22020	65536
Elapsed modeling time	107 s	1652 s
Estimation of the process variance (σ^2)	1.4183	0.0549

TABLE II
Information on the Sentinel-1 Satellite Data Used in This Study

Types of image	Sentinel-1
Number of images	84
Coverage time	2017.03–2019.12
Revisit time	12 days
Number of interferograms	164

segmentation method [see Fig. 7(a) and (b)]. Then, the 164 interferograms are stacked to determine the deformation zone in the interferograms [31] [see Fig. 7(c)]. After masking the deformation zone and low-coherence points, the sampling points in the centers of the quadtree blocks are selected, as shown in Fig. 7(d). Considering the vertically stratified atmosphere and the spatial correlation of the horizontally turbulent atmosphere, a regression model and a variogram model are built, thereby inputting the tropospheric phase into an advanced universal kriging interpolation model. After interpolating all the interferograms, the atmospheric phase of each interferogram is estimated. Then, the interpolation phase is subtracted from the unwrapped phase to obtain the deformation information.

B. Results and Analysis

We estimate all the interferometric pairs by using the proposed method and choose some interferometric pairs to illustrate the results (see Fig. 8). The estimated atmospheric phase reflects

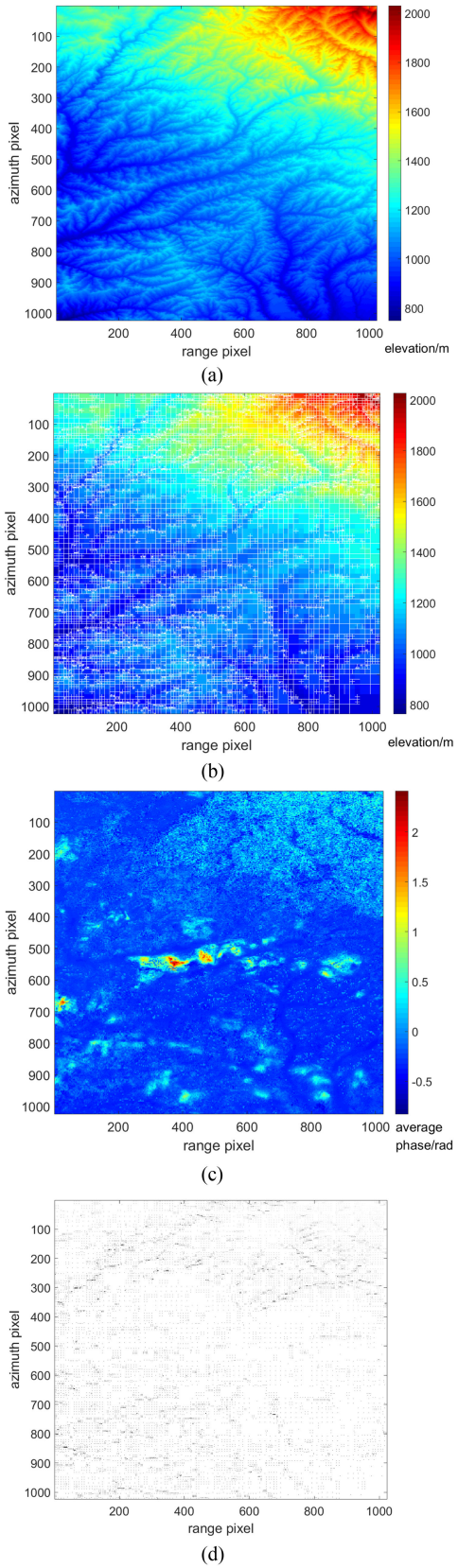

Fig. 7. Schematic diagram of quadtree segmentation. (a) DEM of the study area. (b) DEM after quadtree segmentation. (c) Average interferometric phase. The deformation zones are shown as yellow regions. (d) Map of the sampling points after quadtree segmentation. This method employs nonuniform sampling; the white background indicates null data.

TABLE III
COMPARISON OF THE DIFFERENT ATMOSPHERIC CORRECTION MODELS

Method	Characteristic	Mean of STD of each interferograms
GACOS	Online application	2.06 rad
GAMMA atm model1	Regression analysis of elevation	1.0117 rad
GAMMA atm model2	Regression analysis of elevation with multiple parameters	1.1042 rad
NVCE	Stochastic model	2.52 rad
IPTA	Multi step time consuming operation	0.80 rad
The proposed method	Unified short time operation	0.86 rad

the high potential relativity of the topography, which meets the abovementioned atmospheric characteristics. In addition, we compare the pixel scattering in the interferograms with the same rows and columns of the estimated atmospheric phase and the corrected unwrapped phase. The results are shown in Fig. 9. As mentioned above and shown in Fig. 3, pixel scattering shows an intrinsic tendency toward a three-dimensional position. After correction, the results fluctuate around the true value.

To verify the results, we select three typical areas, which include plain area, deformation area, and mountainous area, to show the correction effects. Then we illustrate the phase value of the different areas in the research zone after the atmospheric phase correction by the proposed method (see Fig. 10). From the histogram of different colors, the initial phase represented by the blue histograms decreases and approaches zero. GAMMAatmmod1 refers to the single patch of the linear atmospheric phase model with the DEM, GAMMAatmmod2 refers to the adaptive two-dimensional atmospheric phase model, the initial phase refers to the unwrapped phase after extracting the topographic phase and flattened phase, and network-based variance-covariance estimation (NVCE) is the method proposed by Li *et al.* and Cao *et al.* The results show that the proposed method has a lower mean value and standard deviation, indicating that the proposed method is beneficial for atmospheric phase correction in TS-InSAR. Besides, to verify the stability of the proposed method, we compare the phase standard deviation in each interferogram without the deformation region by these methods (see Table III). The proposed method shows almost the same stability as IPTA.

After singular value decomposition, we compare the results with the IPTA time-series process (see Fig. 11). The IPTA process includes a multiple pointwise regression of the baseline and time interval of the interferometric phase with a height correction estimation and linear deformation rate estimation. The quality of each regression is measured by the standard deviation. The standard deviation of the final regression is less than 1 rad. The residual atmospheric phase is interpolated by

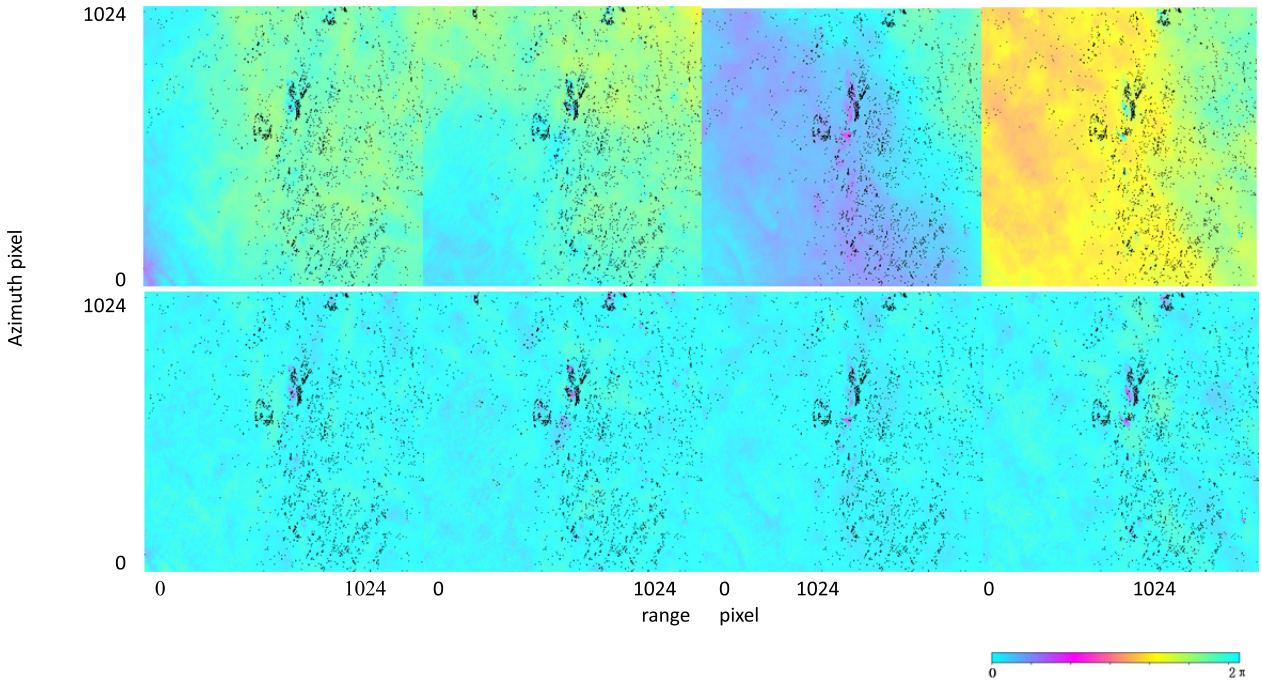

Fig. 8. Corrected interferograms by the proposed method. (a) Estimated atmospheric phase. (b) Unwrapped interferograms after correction by the proposed method.

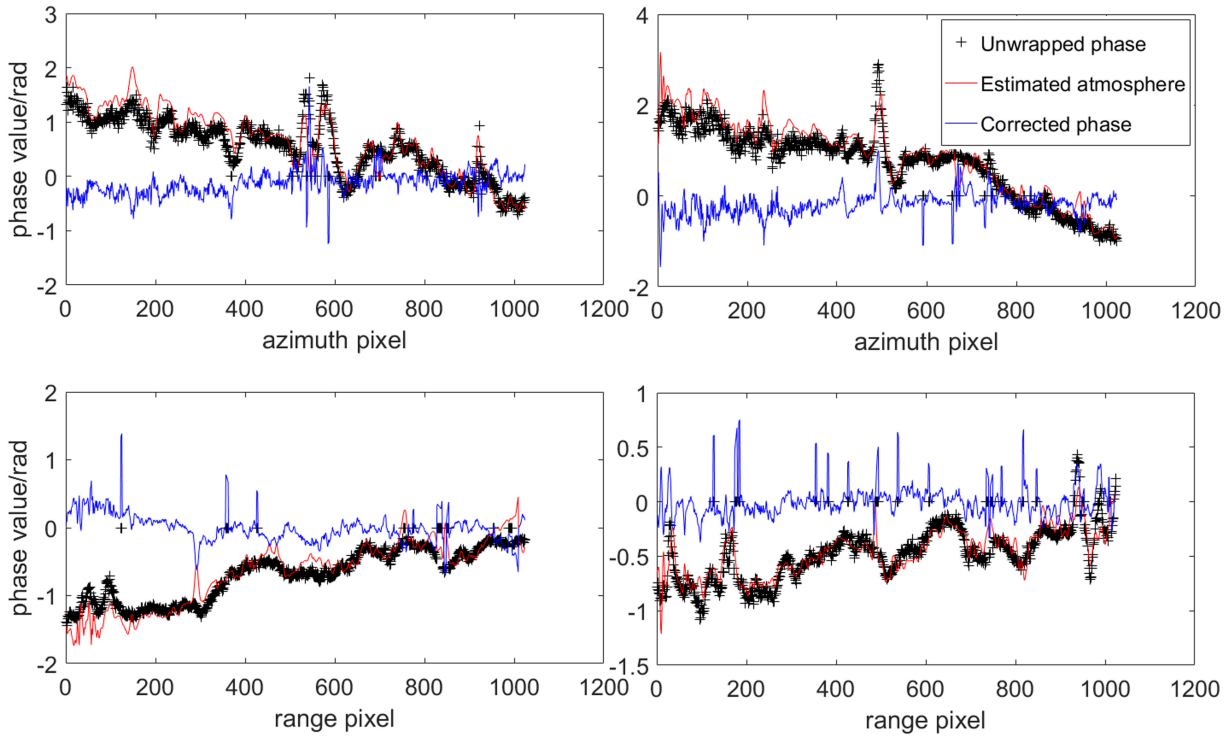

Fig. 9. Scatter diagrams of pixels in the azimuth and range directions. The black crosses indicate the unwrapped phase; the red line indicates the estimated atmospheric phase; and the blue line indicates the corrected unwrapped phase.

spatial filtering with a linear LS filter and IDW interpolation in different windows. Compared with the proposed method, the abovementioned IPTA process is time-consuming and requires manual experience. The proposed method and IPTA both show high consistency in the detection of subsidence areas. However, there are some differences in deformation edge [see Fig. 11(c), (e)] and valley areas [see Fig. 11(d) and (f)] because the interpolation window of IDW is constant and the extent of the residual atmosphere effect is less than the size of the filter window. The solution is increasing the number of

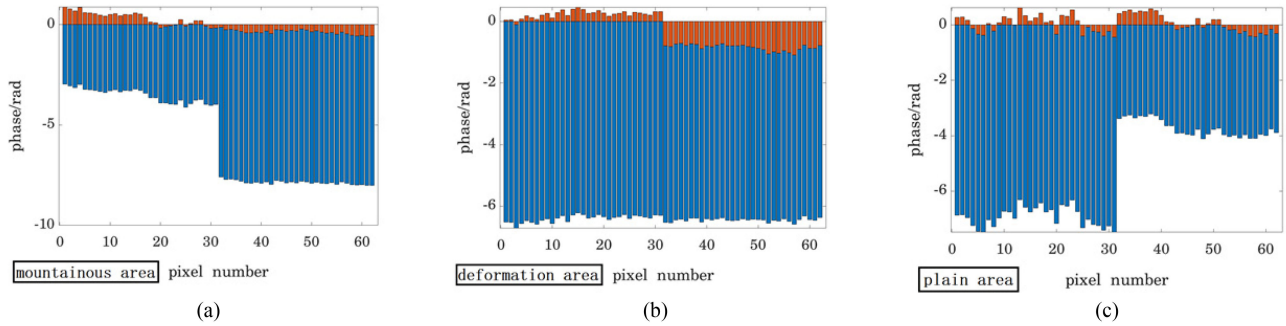

Fig. 10. Phase value of the different areas in the research zone after the atmospheric phase correction by the proposed method.

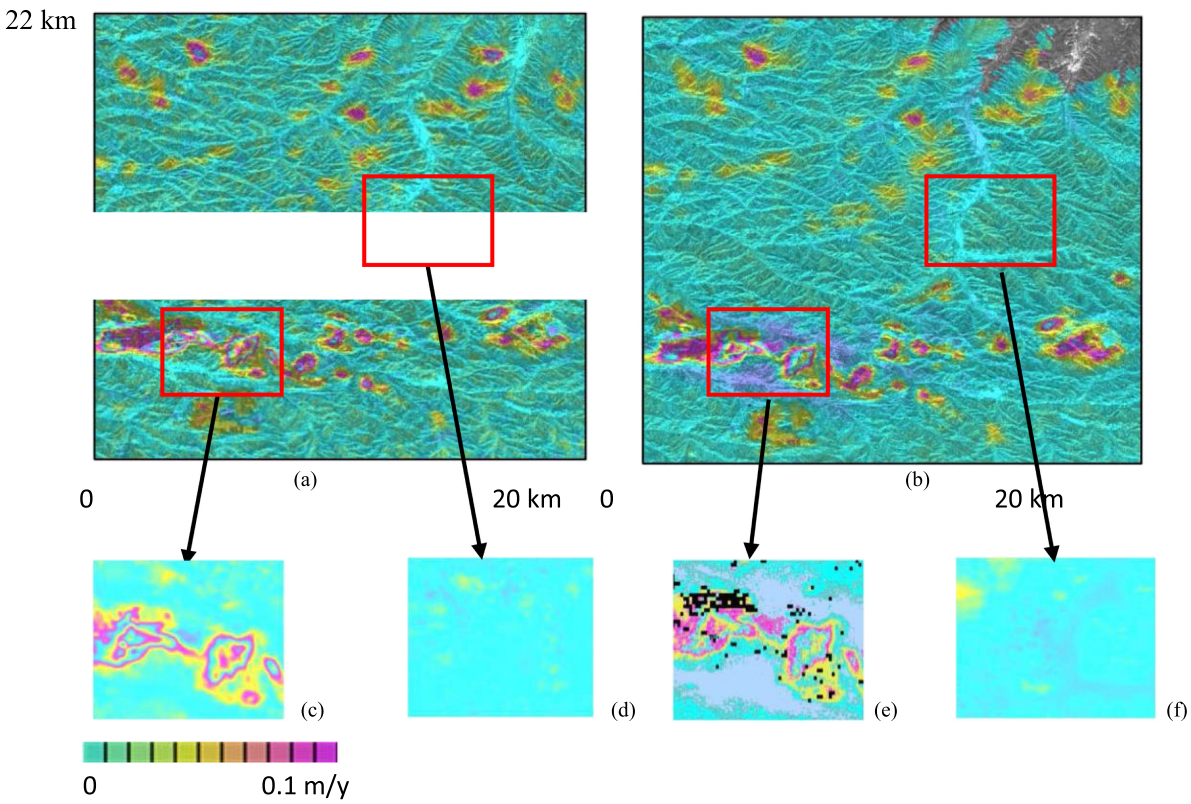

Fig. 11. Comparison of Sentinel-1 data between the IPTA method and the proposed method. (a) Mean rate of deformation by the proposed method. (b) IPTA result. (c)–(f) Local enlarged maps.

iterations by changing the interpolation window size to reduce the atmospheric effects step by step, which is time-consuming and requires processing experience to a certain extent.

IV. Discussion

This article fully considers the characteristics of the troposphere and proposes a method combining quadtree segmentation with universal kriging for tropospheric correction under the TS-InSAR framework. The proposed method can estimate the atmospheric delay from every unwrapped interferometric phase in mountainous areas. The key step of the proposed method relies on the quadtree segmentation model, which divides the DEM into sampling points according to the elevation gradient and improves the universal kriging model with a drift function considering the drift in the range, azimuth, and vertical directions. Moreover, the selection of variogram models is performed based on the characteristics of the atmospheric turbulence phase.

In the experiment, Sentinel-1 images forming 164 interferometric pairs are utilized to mitigate the atmospheric delay by the proposed method, and the results are compared with those of IPTA, NCVE, GACOS, and other GAMMA atmospheric phase models. The differences indicate the advantages of the proposed method in atmospheric correction.

Notably, the proposed method focuses on every interferogram due to the variability of atmospheric conditions. Compared with the traditional time-series processing method, the

proposed method applies improved universal kriging interpolation instead of IDW interpolation based merely on the phase value to estimate the tropospheric delay and considers the spatial correlation and makes unbiased optimal estimations of the local atmospheric phase. In addition, the proposed method utilizes the quadtree segmentation method to divide the typical topography and reduce information redundancy. Compared with conventional moving-window uniform sampling, the proposed method improves the operation efficiency of kriging interpolation, considerably reducing the computation time.

In mountainous areas, the corrected unwrapped phase is affected by the conditions of the unwrapping process and decorrelation. Considering the wide area featuring insignificant deformation, the proposed method needs to be further improved, or the circumstances need to be discriminated and reduced before applying the methodology presented in this paper. We plan to improve the algorithm in our future work to achieve adaptive estimation with high accuracy.

ACKNOWLEDGMENT

The authors would like to thank the European Space Agency for Sentinel-1 data.

REFERENCES

[1] K. Deng, Z. Tan, Y. Jiang, H. Dai, Y. Shi, and L. Xu, *Deformation Monitoring and Subsidence Engineering*. Xuzhou, China: China Univ. Mining Technol. Press, 2014.

[2] R. Goldstein, "Atmospheric limitations to repeat-track radar interferometry," *Geophysical Res. Lett.,* vol. 22, no. 18, pp. 2517–2520, Mar. 1995, doi: 10.1029/95GL02475.

[3] H. A. Zebker, P. A. Rosen, and S. Hensley, "Atmospheric effects in interferometric synthetic aperture radar surface deformation and topographic maps," *J. Geophysical Res. Solid Earth,* vol. 102, no. B4, pp. 7547–7563, Apr. 1997, doi: 10.1029/96JB03804.

[4] S. Aguemoune, A. Ayadi, A. Belhadj-Aissa, and M. Bezzeghoud, "A novel interpolation method for InSAR atmospheric wet delay correction," *J. Appl. Geophys.*, vol. 163, pp. 96–107, 2019, doi: 10.1016/j.jappgeo.2019.02.013.

[5] Z. Hu and J. J. Mallorquí, "An accurate method to correct atmospheric phase delay for InSAR with the ERA5 global atmospheric model," *Remote Sens.*, vol. 11, no. 17, 2019, Art. no. 1969, doi: 10.3390/rs11171969.

[6] C. Yu, Z. Li, and N. T. Penna, "Interferometric synthetic aperture radar atmospheric correction using a GPS-based iterative tropospheric decomposition model," *Remote Sens. Environ.,* vol. 204, pp. 109–121, Jan. 2018, doi: 10.1016/j.rse.2017.10.038.

[7] C. Yu, N. T. Penna, and Z. Li, "Generation of real-time mode high-resolution water vapor fields from GPS observations," *J. Geophysical Res., Atmospheres*, vol. 122, pp. 2008–2025, 2017.

[8] P. Berardino, G. Fornaro, R. Lanari, and E. Sansosti, "A new algorithm for surface deformation monitoring based on small baseline differential SAR interferograms," *IEEE Trans. Geosci. Remote Sens.,* vol. 40, no. 11, pp. 2375–2383, Aug. 2002.

[9] C. Yu, Z. Li, N. T. Penna, and P. Crippa, "Solid earth generic atmospheric correction model for interferometric synthetic aperture radar observations," *J. Geophys. Res. Solid Earth Res.*, vol. 123, pp. 9202–9222, 2018.

[10] A. Ferretti, C. Prati, and F. Rocca, "Permanent scatterers in SAR interferometry," *IEEE Trans. Geosci. Remote Sens.,* vol. 39, no. 1, pp. 8–20, Aug. 2001.

[11] J. Xu, Z. Q. Guan, X. F. He, and J. L. Wang, "Spatial interpolation methods for correcting atmospheric effects using interferometric SAR," *J. Electron. Inf. Technol.,* vol. 30, pp. 911–915, Apr. 2008, doi: 10.3724/SP.J.1146.2006.01684.

[12] Z. Li, J. P. Muller, P. Cross, P. Albert, J. Fischer, and R. Bennartz, "Assessment of the potential of MERIS near-infrared water vapour products to correct ASAR interferometric measurements," *Int. J. Remote Sens.,* vol. 27, no. 2, pp. 349–365, Jan. 2006, doi: 10.1080/01431160500307342.

[13] E. Pichelli *et al.*, "Water vapor distribution at urban scale using high-resolution numerical weather model and spaceborne SAR interferometric data," *Natural Hazards Earth Syst. Sci.,* vol. 10, pp. 121–132, Jan. 2010, doi: 10.5194/nhess-10-121-2010.

[14] P. W. Webley, R. M. Bingley, A. H. Dodson, G. Wadge, S. J. Waugh, and I. N. James, "Atmospheric water vapour correction to InSAR surface motion measurements on mountains: Results from a dense GPS network on mount Etna," *Phys. Chem. Earth, A/B/C,* vol. 27, no. 4, pp. 363–370, Jan. 2002, doi: 10.1016/S1474-7065(02)00013-X.

[15] Z. W. Li *et al.*, "Correcting atmospheric effects on InSAR with MERIS water vapour data and elevation-dependent interpolation model," *Geophysical J. Int.,* vol. 189, no. 2, pp. 898–910, May 2012, doi: 10.1111/j.1365-246X.2012.05432. x.

[16] W. B. Xu, Z. W. Li, X. L. Ding, and J. J. Zhu, "Interpolating atmospheric water vapor delay by incorporating terrain elevation information," *J. Geodesy,* vol. 85, no. 9, pp. 555–564, Sep. 2011, doi: 10.1007/s00190-011-0456-0.

[17] S. Knospe and S. Jonsson, "Covariance estimation for dInSAR surface deformation measurements in the presence of anisotropic atmospheric noise," *IEEE Trans. Geosci. Remote Sens.,* vol. 48, no. 4, pp. 2057–2065, Aug. 2010.

[18] S. H. Hong, S. Wdowinski, S. W. Kim, and J. S. Won, "Multitemporal monitoring of wetland water levels in the Florida everglades using interferometric synthetic aperture radar (InSAR)," *Remote Sens. Environ.,* vol. 114, no. 11, pp. 2436–2447, Nov. 2010, doi: 10.1016/j.rse.2010.05.019.

[19] R. F. Hanssen, *Radar Interferometry: Data Interpretation and Error Analysis*. Dordrecht, The Netherlands: Springer, 2001.

[20] J. Wei, Z. Li, J. Hu, G. Feng, and M. Duan, "Anisotropy of atmospheric delay in InSAR and its effect on InSAR atmospheric correction," *J. Geodesy,* vol. 93, no. 2, pp. 241–265, Feb. 2019, doi: 10.1007/s00190-018-1155-x.

[21] Z. Li *et al.*, "Time-series InSAR ground deformation monitoring: Atmospheric delay modeling and estimating," *Earth Sci. Rev.,* vol. 192, pp. 258–284, May 2019, doi: 10.1016/j.earscirev.2019.03.008.

[22] Y. Cao, Z. Li, J. Wei, J. Hu, M. Duan, and G. Feng, "Stochastic modeling for time series InSAR: With emphasis on atmospheric effects," *J. Geodesy,* vol. 92, no. 2, pp. 185–204, Feb. 2018, doi: 10.1007/s00190-017-1055-5.

[23] R. Bamler and P. Hartl, "Topical Review: Synthetic aperture radar interferometry," *Inverse Probl.,* vol. 14, no. 4, p. 1, Jul. 1998, doi: 10.1088/0266-5611/14/4/001.

[24] C. Werner, U. Wegmuller, T. Strozzi, and A. Wiesmann, "Interferometric point target analysis for deformation mapping," in *Proc. IGARSS IEEE Int. Geosci. Remote Sens. Symp.*, Toulouse, France, 2004, pp. 4362–4364.

[25] U. Wegmuller, D. Walter, V. Spreckels, and C. L. Werner, "Nonuniform ground motion monitoring with TerraSAR-X persistent scatterer interferometry," *IEEE Trans. Geosci. Remote Sens.,* vol. 48, no. 2, pp. 895–904, Nov. 2010.

[26] M. Costantini, F. Minati, A. Quagliarini, and G. Schiavon, "SAR interferometric baseline calibration without need of phase unwrapping," in *Proc. IGARSS IEEE Int. Geosci. Remote Sens. Symp.*, Anchorage, AK, USA, 2004, pp. 493–495.

[27] M. Taylor and G. Peltzer, "Current slip rates on conjugate strike-slip faults in central Tibet using synthetic aperture radar interferometry," *J. Geophysical Res. Solid Earth,* vol. 111, no. B12, Dec. 2006, Art. no. B12402, doi: 10.1029/2005JB004014.

[28] X. L. Ding, Z. W. Li, J. J. Zhu, G. C. Feng, and J. P. Long, "Atmospheric effects on InSAR measurements and their mitigation," *Sensors (Basel),* vol. 8, no. 9, pp. 5426–5448, Sep. 2008, doi: 10.3390/s8095426.

[29] S. Baffelli, O. Frey, and I. Hajnsek, "Geostatistical analysis and mitigation of the atmospheric phase screens in ku-band terrestrial radar interferometric observations of an alpine glacier," *IEEE Trans. Geosci. Remote Sens.*, vol. 58, no. 11, pp. 7533–7556, Nov. 2020.

[30] N. D. Le and J. V. Zidek, *Statistical Analysis of Environmental Space-Time Processes*. Dordrecht, The Netherlands: Springer, 2006.

[31] H. Liang, L. Zhang, X. Ding, Z. Lu, and X. Li, "Toward mitigating stratified tropospheric delays in multitemporal InSAR: A quadtree aided joint model," *IEEE Trans. Geosci. Remote Sens.,* vol. 57, no. 1, pp. 291–303, Aug. 2019.

[32] M. A. Siddique, T. Strozzi, I. Hajnsek, and O. Frey, "A case study on the correction of atmospheric phases for SAR tomography in mountainous regions," *IEEE Trans. Geosci. Remote Sens.*, vol. 57, no. 1, pp. 416–431, Jan. 2019.

[33] C. Esch *et al.*, "On the analysis of the phase unwrapping process in a D-InSAR stack with special focus on the estimation of a motion model," *Remote Sens.*, 2019, vol. 11, no. 19, Art. no. 2295, doi: 10.3390/rs11192295.

Mengyao Shi received the B.S. degree in resource exploration engineering and the M.S. degree in surveying and mapping in 2017 and 2018, respectively, from the China University of Geosciences, Beijing, China, where he has been working toward the Ph.D. degree in InSAR data processing and geohazard monitoring since 2018.

Junhuan Peng was born in Chongqing, China, in 1964. He received the B.S. degree in surveying and mapping and the M.S. degree in mine surveying from Central South University, Changsha, China, in 1985 and 1988, respectively, and the Ph.D. degree in geodesy and surveying engineering from Wuhan University, Wuhan, China, in 2003.

From 1988 to 2003, he was with the Guilin University of Technology as a Lecturer and then as a Professor. From 2003 to 2005, he was a Postdoctoral Researcher in geodesy and surveying engineering with Shanghai Astronomical Observatory, China Academy of Sciences, Shanghai, China. From 2005 to 2007, he was with Chongqing University as a Professor. Since 2007, he has been working as a Full Professor with the China University of Geosciences, Beijing, China. He has served as a Reviewer for several famous surveying and mapping and related academic journals and has authored/coauthored more than 40 papers in Chinese and English in both international and national journals.

Xue Chen received the M.Eng. degree in geomatics engineering from the China University of Geosciences, Beijing, China, in 2014. She is currently working toward the Ph.D. degree with the China University of Geosciences and the University of Padua, Padua, Italy.

Her research focuses on the use of radar interferometry to study geohazards.

Yueze Zheng received the B.S. degree in surveying engineering from Inner Mongolia Normal University, Huhehot, China, in 2016, and the M.S. degree in surveying and mapping from the China University of Geosciences, Beijing, China, in 2019.

Since 2019, he has been working with the Beijing Institute of Surveying and Mapping, Beijing, China, with a focus on remote sensing monitoring.

Honglei Yang received the B.S. degree in surveying and mapping from the Information Engineering University, Zhengzhou, Henan, in 2006 and the M.S. and Ph.D. degrees in cartography and geographical information engineering from the China University of Geosciences, Beijing, China, in 2009 and 2012, respectively.

From 2012 to 2014, he was with the China University of Geosciences as a Postdoctoral Researcher. Since 2014, he has been working with the China University of Geosciences. He has authored/coauthored 20 papers in Chinese and English in both international and national journals.

Yuhan Su is currently working toward the Ph.D. degree with the School of Land Science and Technology, China University of Geosciences, Beijing, China.

His research interests include interferometric synthetic aperture radar data processing methods and their application in the study of natural hazards.

Guoya Wang received the B.S. degree in surveying engineering from the Guilin University of Technology, Guilin, China, in 1997 and the M.S. and Ph.D. degrees in physical geography from the Cold and Arid Regions Engineering Institute, Chinese Academy of Sciences, Lanzhou, China, in 2007 and 2010, respectively.

Since 2010, she has been working on cryosphere hydrology and the prevention and control of geological disasters, and she has authored/coauthored more than 15 papers in Chinese and English in both international and national journals. Since 2012, she has been an Associate Researcher with the Geological Hazards Prevention Institute, Gansu Academy of Sciences, Gansu, China.

Wenwen Wang received the B.S. degree in geoinformation from the North China University of Science and Technology, Tangshan, Hebei, China, in 2010, and the M.S. degree in geological engineering from the University of Geosciences, Beijing, China, in 2013.

Since 2013, she has been working with the Coal Geological Geophysical Exploration Surveying and Mapping. Institute of Shanxi Province with a focus on general surveys of geographical conditions, national land surveys, and remote sensing surveys of environmental geology in Shanxi Province, China.